ARTICLE

Effective hematopoietic stem cell-based gene therapy in a murine model of hereditary pulmonary alveolar proteinosis

Miriam Hetzel,[1] Elena Lopez-Rodriguez,[2] Adele Mucci,[1] Ariane Hai Ha Nguyen,[1] Takuji Suzuki,[3,4] Kenjiro Shima,[3] Theresa Buchegger,[1] Sabine Dettmer,[5] Thomas Rodt,[5] Jens P. Bankstahl,[6] Punam Malik,[7] Lars Knudsen,[2] Axel Schambach,[1,8] Gesine Hansen,[9] Bruce C. Trapnell,[3,10] Nico Lachmann[1*] and Thomas Moritz[1*]

[1]Institute of Experimental Hematology, Hannover Medical School, Hannover, Germany; [2]Institute of Functional and Applied Anatomy, Hannover Medical School, Hannover, Germany; [3]Translational Pulmonary Science Center, Division of Pulmonary Biology, Cincinnati Children's Hospital Medical Center, Cincinnati, OH, USA; [4]Division of Pulmonary Medicine, Jichi Medical University, Shimotsukeshi, Tochigi, Japan; [5]Department of Radiology, Hannover Medical School, Hannover, Germany; [6]Department of Nuclear Medicine, Hannover Medical School, Hannover, Germany; [7]Division of Experimental Hematology and Cancer Biology, Cancer and Blood Disease Institute (CBDI), Cincinnati Children's Hospital Medical Center, Cincinnati, OH, USA; [8]Division of Hematology/Oncology, Boston Children's Hospital, Harvard Medical School, Boston, MA, USA; [9]Department of Pediatrics, Allergology, and Neonatology, Hannover Medical School, Hannover, Germany and [10]Division of Pulmonary Medicine, Children's Hospital Medical Center, Cincinnati, OH, USA

NL and TM contributed equally to this work.

Ferrata Storti Foundation

Haematologica 2020
Volume 105(4):1147-1157

ABSTRACT

Hereditary pulmonary alveolar proteinosis due to GM-CSF receptor deficiency (herPAP) constitutes a life-threatening lung disease characterized by alveolar deposition of surfactant protein secondary to defective alveolar macrophage function. As current therapeutic options are primarily symptomatic, we have explored the potential of hematopoietic stem cell-based gene therapy. Using *Csf2rb*$^{-/-}$ mice, a model closely reflecting the human herPAP disease phenotype, we here demonstrate robust pulmonary engraftment of an alveolar macrophage population following intravenous transplantation of lentivirally corrected hematopoietic stem and progenitor cells. Engraftment was associated with marked improvement of critical herPAP disease parameters, including bronchoalveolar fluid protein, cholesterol and cytokine levels, pulmonary density on computed tomography scans, pulmonary deposition of Periodic Acid-Schiff^{+} material as well as respiratory mechanics. These effects were stable for at least nine months. With respect to engraftment and alveolar macrophage differentiation kinetics, we demonstrate the rapid development of CD11c^{+}/SiglecF^{+} cells in the lungs from a CD11c^{-}/SiglecF^{+} progenitor population within four weeks after transplantation. Based on these data, we suggest hematopoietic stem cell-based gene therapy as an effective and cause-directed treatment approach for herPAP.

Introduction

Hereditary pulmonary alveolar proteinosis (herPAP) represents an extremely rare life-threatening genetic disorder associated with malfunction of alveolar macrophages (AM).[1] HerPAP is caused by mutations in genes encoding the granulocyte/macrophage-colony-stimulating factor receptor (GM-CSFR), a high-affinity receptor complex composed of a cytokine-specific α (GM-CSFRα, *CSF2RA*) and a signal-transducing common β (GM-CSFRβ, *CSF2RB*) chain shared with the IL-3

Correspondence:

THOMAS MORITZ
moritz.thomas@mh-hannover.de

Received: December 17, 2018.

Accepted: July 5, 2019.

Pre-published: July 9, 2019.

doi:10.3324/haematol.2018.214866

Check the online version for the most updated information on this article, online supplements, and information on authorship & disclosures: www.haematologica.org/content/105/4/1147

©2020 Ferrata Storti Foundation

Material published in Haematologica is covered by copyright. All rights are reserved to the Ferrata Storti Foundation. Use of published material is allowed under the following terms and conditions: https://creativecommons.org/licenses/by-nc/4.0/legalcode. Copies of published material are allowed for personal or internal use. Sharing published material for non-commercial purposes is subject to the following conditions: https://creativecommons.org/licenses/by-nc/4.0/legalcode, sect. 3. Reproducing and sharing published material for commercial purposes is not allowed without permission in writing from the publisher.

and IL-5 receptor. Although the GM-CSFR is expressed on a wide variety of hematopoietic cells, mutations in either *CSF2RA*[2,3] or *CSF2RB*[4,5] almost exclusively affect the maturation and functionality of AM, leading to disturbed intracellular surfactant degradation, intrapulmonary deposition of phospholipids and lipoproteins, and, in turn, severe respiratory insufficiency. Current treatment options are symptomatic only and consist of vigorous treatment of pulmonary infections and whole lung lavage, a highly invasive procedure performed under general anesthesia, which may need to be repeated every 4-8 weeks. As for other hereditary diseases affecting the lymphohematopoietic system, allogeneic hematopoietic stem cell transplantation (alloHSCT) or hematopoietic stem cell-based gene therapy (HSC-GT) using retroviral vectors[6,7] potentially offer a permanent cure for herPAP patients and proof of concept for these concepts has been established in murine models.[8,9] However, in the clinical setting, both procedures are problematic due to the required chemo/radiotherapeutic preconditioning and the poor pulmonary status of herPAP patients.[3] On the other hand, over the last decade, substantial progress has been made in the fields of alloHSCT as well as HSC-GT, and in this context, successful alloHSCT has recently been reported in two patients suffering from secondary PAP[10] as well as in a herPAP patient.[11]

In addition, novel treatment strategies for herPAP are evolving. Thus, the direct intrapulmonary application of macrophages (pulmonary macrophage transplantation; PMT) has demonstrated profound and long-lasting therapeutic efficacy in two murine models of herPAP in the absence of any preconditioning.[12-16] While it is not clear yet whether in the human setting these pulmonary administered macrophages will permanently persist in the lungs and provide a long-term cure for herPAP patients, PMT might still improve the patients' general condition to allow for a more permanent approach such as alloHSCT or HSC-GT.

On this background, we here employed a state-of-the-art, 3rd generation self-inactivating (SIN) lentiviral vector and transduced lineage-negative hematopoietic stem and progenitor cells (lin$^-$ HSPC) derived from the bone marrow (BM) of *Csf2rb*$^{-/-}$ mice[17] to evaluate the feasibility and efficacy of an HSC-GT strategy for herPAP *in vivo*. In this study, we demonstrated robust and long-term pulmonary engraftment of AM which was associated with significant improvements of critical disease-related parameters such as elevated protein, cholesterol, or cytokine levels in the alveolar spaces. In addition, our study offers novel insights into the early reconstitution phase of a functional AM compartment following HSCT.

Methods

Mice

B6.SJL-Ptprca-Pep3b/BoyJZtm (Ly5.1; CD45.1) mice were used as wild-type (WT) controls, and B6;129P2-Csf2rb2^{tm1Mur} (*Csf2rb*$^{-/-}$) harboring a knockout in the *Csf2rb* gene served as a disease model of PAP. Mice were housed in the central animal facility of Hannover Medical School under specific-pathogen-free conditions in individually ventilated cages (IVC). Mice had access to food and water *ad libitum*. All animal experiments were approved by the Lower Saxony State animal welfare committee and were conducted according to the law governing animal welfare.

Isolation, cultivation, and transduction of lineage negative cells

Lineage negative cells were isolated from total bone marrow using lineage cell depletion kit (Miltenyi) following the manufacturer's instructions. Pre-stimulation of lineage negative cells was performed for 24 hours in STIF medium (StemSpan medium supplemented with 1mM Penicillin/Streptomycin, 2mM L-glutamine, 100 ng/mL mSCF, 20 ng/mL TPO, 20 ng/mL IGF-2 and 100 ng/mL FGF2). Following this, transduction of lineage negative cells was performed on RetroNectin® (Takara) coated plates using STIF medium and MOI between 10 and 20, as previously described.[18] For *in vitro* assays, cells were sorted for GFP expression using a FACSAria IIu.

Hematopoietic stem cell transplantation

Age-matched (12-16 week old) *Csf2rb*$^{-/-}$ recipient mice of both sexes were irradiated with a single dose of 9 Gy. Lin$^-$ BM cells of wild-type (WT) donor mice were isolated as described above and injected intravenously into the tail vein of recipient mice 24 hours post irradiation. Alternatively, lineage negative cells of *Csf2rb*$^{-/-}$ donor mice were isolated and transduced with SIN lentiviral gene therapy or GFP control vectors and transplanted by the same protocol. In secondary transplantation, BM of primary recipients was isolated, red blood cell lysis performed and subsequently, cells were injected by the same protocol as described above. For all experiments, non-sex- and non-age-matched (age ≤9 months), non-irradiated *Csf2rb*$^{-/-}$ and WT mice served as reference controls.

Bronchoalveolar lavage

After closing the left lung, the right lung was flushed three times with PBS (once with 0.6 mL and 2 times with 0.5 mL) to obtain bronchoalveolar lavage fluid (BALF). The turbidity of the fluid was measured by analyzing the OD600 value on a BioPhotometer (Eppendorf). The protein concentration of total BALF was analyzed using the Pierce™ BCA Protein Assay Kit (Thermo Fisher Scientific) according to the manufacturer's instructions. BALF samples were pelleted for 10 minutes at 400xg. Supernatants were used to determine the concentration of GM-CSF, M-CSF, and MCP-1 by ELISA (Mouse Quantikine Kits, R&D Systems), as described.[2] Cholesterol levels were measured by the amplex red cholesterol assay (Life Technologies) according to the manufacturer's protocol, as described.[19] Pelleted cells were stained and analyzed by flow cytometry using BD LSR II.

Statistical analysis

Statistical analysis was performed using the Prism 7 software (GraphPad) applying ANOVA and recommended *post hoc* testing. Unless otherwise stated, bars and average numbers in the text represent mean±standard error of mean (SEM).

Results

Lentiviral transduction restores GM-CSFRβ expression and GM-CSF-dependent functionality in *Csf2rb*$^{-/-}$ hematopoietic stem and progenitor cells and macrophages *in vitro*

A 3rd generation SIN lentiviral vector constitutively expressing murine *Csf2rb* cDNA from an elongation factor 1 α (EF1 α) promoter (Lv.Csf2rb) was employed, and for better visualization upon flow cytometry, an enhanced GFP (eGFP) reporter coupled to the transgene via an inter-

nal ribosomal entry site (IRES) was added (*Online Supplementary Figure S1A*). The construct was used to transduce lin⁻ HSPC from B6;129P2-Csf2rb2tm1Mur (*Csf2rb*$^{-/-}$) mice. These mice harbor a knock out in the *Csf2rb* gene and closely reflect the clinical herPAP disease phenotype.[17] Following HSPC transduction, robust GFP reporter expression (Figure 1A), as well as surface expression of the GM-CSFRβ chain (CD131) (Figure 1B), was observed. Of note, *Csf2rb*$^{-/-}$ lin⁻ cells contained a small population of CD131^{+} cells, most likely due to the additional and highly similar IL-3 specific β-chain present in mice[20] that is intact in *Csf2rb*$^{-/-}$ mice as well. When subjecting Lv.Csf2rb-transduced HSPC that were previously sorted for GFP^{+} cells to a colony assay with GM-CSF added as the only cytokine, significant restoration of GM-CSF-dependent colony formation was observed (WT 24±4, Lv.Csf2rb 17±6, *Csf2rb*$^{-/-}$ 0±0, mean±SEM) (Figure 1C) with colonies displaying similar morphologies as those derived from WT cells (*Online Supplementary Figure S1B* and *C*). No significant difference in colony numbers (WT 72±20, Lv.Csf2rb 38±8, *Csf2rb*$^{-/-}$ 71±11, mean±SEM) or morphology between Lv.Csf2rb-transduced and non-transduced

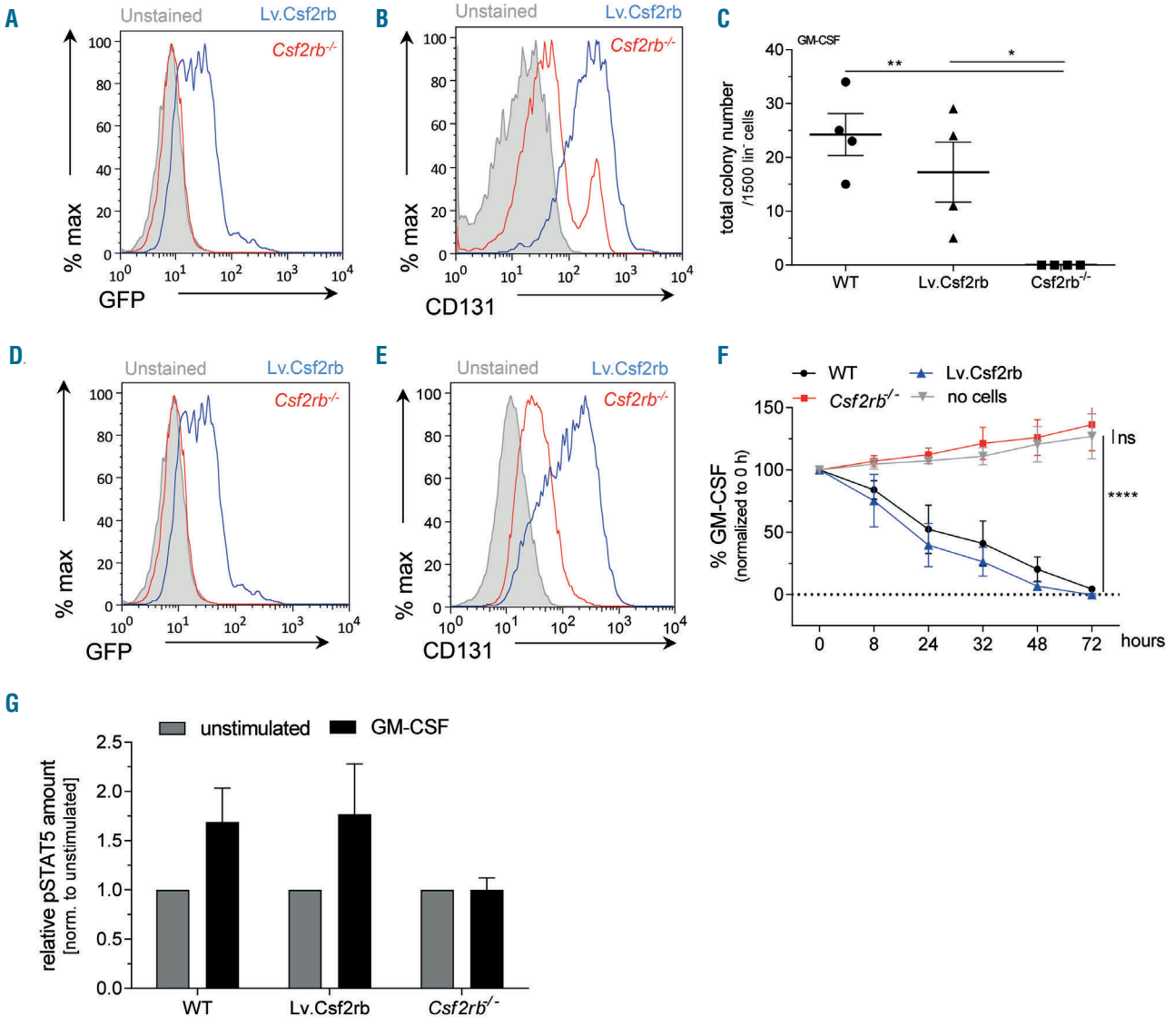

Figure 1. Lv.Csf2rb-transduction of *Csf2rb*$^{-/-}$ cells restores granulocyte/macrophage-colony-stimulating factor (GM-CSF)-dependent functionality of hematopoietic stem and progenitor cells (HSPC) and HSPC-derived macrophages. (A and B) Representative histograms depicting GFP (A) and CD131 (B) expression in hematopoietic stem and progenitor cells (HSPC). (C) Methylcellulose-based clonogenic colony growth in response to GM-CSF. Total colony number per 1,500 lineage negative (lin⁻) HSPC is given. N=2 in technical duplicates; bars indicate mean±standard error of mean (SEM); statistical calculation was done by one-way ANOVA with Dunnett's multiple comparisons test. (D and E) Representative histogram depicting GFP (D) and CD131 (E) expression in macrophages. (F) Clearance of GM-CSF from cell culture supernatant by macrophages. N=3. Data points indicate mean±SEM. Values are normalized to the 0 h time point. Statistical calculation was done by two-way ANOVA with Dunnett's multiple comparisons test. The significance is given for the 72h time point. (G) Increase of phosphorylated STAT5 (pSTAT5) after GM-CSF stimulation. Macrophages were stimulated with GM-CSF for 15 minutes or left without stimulation. Mean fluorescence intensity (MFI) was measured by flow cytometry, and MFI values for stimulated samples were normalized to the corresponding unstimulated sample. N=3. No statistically significant difference. Ns: not significant; *P<0.05; **P<0.01; ****P<0.0001. WT: wild-type.

cells were observed when a cocktail of IL-3, IL-6, SCF, and EPO was applied (*Online Supplementary Figure S1D and E*) demonstrating the GM-CSF specificity of Lv.Csf2rb-mediated effects.

Given that primarily macrophages (MΦ) are affected in herPAP, as a next step, lin$^-$ cells were differentiated towards MΦ *in vitro* by applying M-CSF and assessed for morphology, transgene expression, and GM-CSF-dependent functionality. Typical MΦ morphology similar to WT and *Csf2rb*$^{-/-}$ MΦ was observed for Lv.Csf2rb-transduced MΦ (*Online Supplementary Figure S1F*) and sustained GFP as well as CD131 expression was detected for these cells (Figure 1D and E). Moreover, Lv.Csf2rb-transduced MΦ, in clear contrast to non-transduced *Csf2rb*$^{-/-}$ MΦ, were able to bind and internalize GM-CSF with comparable efficiency as WT MΦ (Figure 1F). In addition, when we analyzed phosphorylation of the signal transducer and activator of transcription 5 (STAT5), a major component in the GM-CSFR signaling cascade, non-transduced *Csf2rb*$^{-/-}$ MΦ failed to phosphorylate STAT5 in response to GM-CSF, whereas STAT5 phosphorylation was restored following Lv.Csf2rb-transduction (Figure 1G).

These data demonstrate that the Lv.Csf2rb vector efficiently directs Csf2rb expression and restores GM-CSF-dependent functionality in *Csf2rb*$^{-/-}$ HSPC as well as thereof derived MΦ, whereas GM-CSF independent properties such as colony formation potential or differentiation properties in response to other cytokines were not affected. Thus, this vector appeared suitable for further evaluation *in vivo*.

Lv.Csf2rb-transduced lin$^-$ hematopoietic stem and progenitor cells engraft in *Csf2rb*$^{-/-}$ mice and reconstitute the hematopoietic system

For *in vivo* evaluation of our construct, we performed HSC-GT employing lethally irradiated *Csf2rb*$^{-/-}$ mice and either the Lv.Csf2rb construct or a control construct harboring GFP only (Lv.GFP) (Figure 2A). A cohort receiving healthy CD45.1$^+$ donor cells served as a positive control. To monitor engraftment and hematopoietic reconstitution, blood samples were taken four, eight, and twelve weeks after HSC-GT, the latter representing the time point of final analysis. Two independent rounds of transplantation were performed with a total of six mice receiving Lv.Csf2rb-

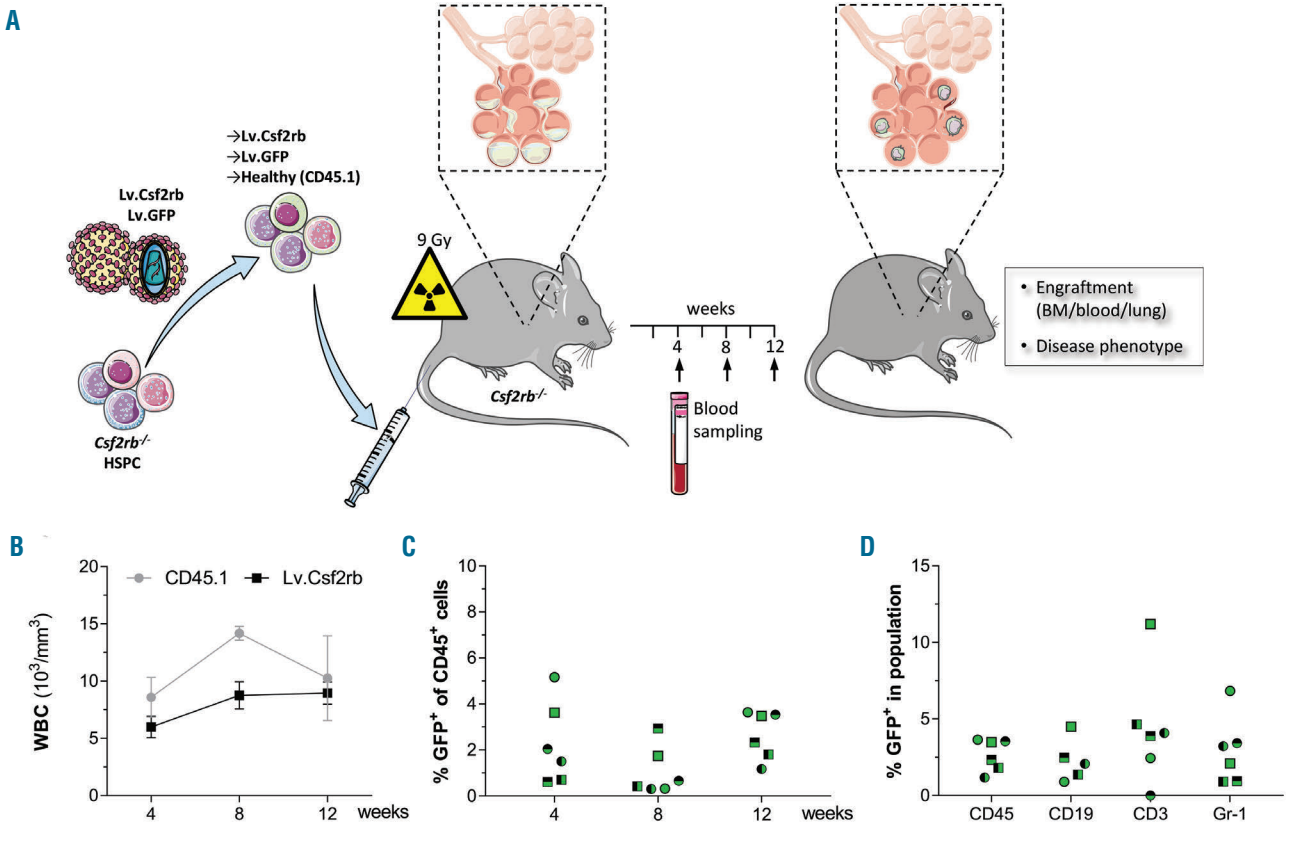

Figure 2. Hematopoietic reconstitution after Lv.Csf2rb hematopoietic stem cell-based gene therapy (HSC-GT). (A) Schematic representation of HSC-GT procedure. *Csf2rb*$^{-/-}$ hematopoietic stem and progenitor cells (HSPC) were isolated from donor mice and transduced with the gene therapy vector (Lv.Csf2rb) or a GFP control vector (Lv.GFP). Lv.Csf2rb-, Lv.GFP-transduced or healthy CD45.1 control HSPC were injected into *Csf2rb*$^{-/-}$ recipients previously lethally irradiated with a single dose of 9 Gy. Blood samples were drawn four, eight and 12 weeks after HSC-GT. The final analysis was performed 12 weeks after HSC-GT to evaluate engraftment of donor cells in bone marrow (BM), blood and lungs as well as to evaluate the reduction of lipoproteinaceous material in the lungs. All images in this illustration were adapted from Servier Medical Art (*https://smart.servier.com*) and are distributed under the CC-BY 3.0 license. (B) Blood count analysis showing total number of white blood cells (WBC) per mm^3 of peripheral blood four, eight and 12 weeks after HSC-GT in mice receiving Lv.Csf2rb-transduced *Csf2rb*$^{-/-}$ cells (black) or healthy CD45.1$^+$ cells (gray); n=6 in two independent experiments. Dots indicate mean±standard error of mean. (C) Percentage of GFP$^+$ cells in peripheral blood CD45$^+$ cells four, eight and 12 weeks after injection of Lv.Csf2rb-transduced cells; n=6 in two independent experiments. Circles belong to the first experiment, squares to the second experiment; equal symbols in (C) and (D) represent the same mice. (D) Percentage of GFP$^+$ cells in peripheral blood CD45$^+$, CD19$^+$, CD3$^+$ and Gr-1$^+$ subsets of mice transplanted with Lv.Csf2rb-transduced cells; n=6 in two independent experiments.

transduced cells, three mice receiving Lv.GFP-transduced cells, and four mice receiving healthy CD45.1$^+$ cells. Hematopoietic reconstitution in mice receiving Lv.Csf2rb-transduced cells was detected already at four weeks ($6.0\pm0.9x10^3/mm^3$ total white blood cells; WBC; mean±SEM), and WBC maintained stably thereafter until week 12 comparable to control mice transplanted with healthy CD45.1$^+$ HSPC (Figure 2B). A clear, though low-level, contribution of Lv.Csf2rb-transduced GFP$^+$ cells was observed during this period (Figure 2C) with a comparable contribution to T, B, and myeloid compartments when analyzed at the week 12 time point (Figure 2D).

Thus, all mice transplanted with Lv.Csf2rb-transduced cells presented effective reconstitution of the hematopoietic system, although at low levels of transduced cells.

Lv.Csf2rb-transduced cells migrate to the lungs and restore the alveolar macrophage pool

In a next step, we evaluated the engraftment of gene-modified cells in the alveolar spaces of *Csf2rb*$^{-/-}$ recipients following HSC-GT. While at the end of the experiment both *Csf2rb*$^{-/-}$ mice and control mice transplanted with Lv.GFP-transduced cells lacked endogenous AM, mice transplanted with Lv.Csf2rb-transduced cells similar to WT mice and controls transplanted with healthy CD45.1$^+$ cells presented a distinct population of Siglec-F$^+$ cells in their lungs, which resided in the alveolar spaces close to the alveolar septa (*Online Supplementary Figure S2A*). To analyze these cells in more detail, homogenized lung tissue was analyzed by flow cytometry (Figure 3A). Cells displaying a CD45$^+$F4/80$^+$Siglec-F$^+$CD11c^{high} phenotype characteristic of mature AM were detected in all mice transplanted with Lv.Csf2rb-transduced cells, similar to control animals receiving healthy CD45.1$^+$ cells or WT mice, while these cells were absent in *Csf2rb*$^{-/-}$ controls or mice transplanted with Lv.GFP-transduced cells (Figure 3B and *Online Supplementary Figure S2B*).

Corresponding results were obtained when the lungs were flushed, and the resulting bronchoalveolar lavage fluid (BALF) was analyzed by flow cytometry. As expected, AM were detected in mice transplanted with Lv.Csf2rb-transduced or healthy CD45.1$^+$ HSPC and in WT mice (Figure 3C and D and *Online Supplementary Figure S2C*). The majority of hematopoietic cells in the BALF of mice transplanted with Lv.Csf2rb-transduced cells was GFP$^+$ and showed robust CD131 expression comparable to mice transplanted with healthy CD45.1$^+$ cells. In contrast, GFP$^+$ cells were almost absent in mice receiving Lv.GFP-transduced cells (Figure 3E and *Online Supplementary Figure S2D*). Vector copy number (VCN) analysis of BALF cells confirmed the presence of genetically modified cells in the lungs of mice receiving Lv.Csf2rb- or Lv.GFP-transduced cells. However, mice receiving Lv.GFP-transduced cells exhibited similar VCN in BM, peripheral blood (PB), or BALF cells (*Online Supplementary Figure S2E*), whereas mice of the Lv.Csf2rb group showed substantially increased VCN in BALF as compared to BM or PB cells (Figure 3F). Enrichment of VCN in BALF *versus* BM cells was up to 16-fold, documenting the enhanced recruitment of corrected cells to the alveolar spaces in the Lv.Csf2rb-transduced cohort.

Taken together, these data demonstrate that, following HSC-GT, in the Lv.Csf2rb group a population of transduced cells migrates to the alveolar spaces and restores the deficient AM pool of *Csf2rb*$^{-/-}$ recipients.

Lv.Csf2rb hematopoietic stem cell-based gene therapy reverses the hereditary pulmonary alveolar proteinosis disease phenotype

A major hallmark of herPAP is the accumulation of surfactant proteins and lipids in the alveolar spaces giving rise to a turbid, milky appearance of the BALF. Following the transplantation of Lv.Csf2rb-transduced HSPC, however, the BALF acquires a clear appearance comparable to WT mice or mice transplanted with healthy CD45.1$^+$ cells (Figure 4A). This initial observation was confirmed by BALF turbidity (OD600 absorbance) and total protein analysis (Figure 4B and C). As the material accumulated in the alveolar spaces is characterized by a high contribution of cholesterol,[19] we also analyzed the cholesterol levels in BALF and detected significant improvements in mice transplanted with Lv.Csf2rb-transduced cells (Figure 4D). Moreover, in *Csf2rb*$^{-/-}$ mice, like in herPAP patients, BALF levels of GM-CSF, M-CSF and MCP-1 are markedly increased due to auto-regulatory mechanisms directed to stabilize the AM population.[1-5,21] While none of these parameters was improved by transplantation of Lv.GFP-transduced cells, twelve weeks after injection of Lv.Csf2rb-transduced cells, all parameters normalized mimicking the situation in WT or CD45.1 transplanted control animals (Figure 4E-G), highlighting the considerable potential of HSC-GT in herPAP.

As a next step, we evaluated lung sections for the deposition of Periodic-Acid Schiff (PAS) positive material. While lungs of untreated *Csf2rb*$^{-/-}$ mice and animals transplanted with Lv.GFP-transduced cells nicely showed the pathognomonic foci of accumulated PAS$^+$ surfactant material, these foci were virtually absent in mice transplanted with Lv.Csf2rb-transduced cells similar to animals of the CD45.1 and WT cohort (*Online Supplementary Figure S3A*). Morphometric quantification confirmed the pronounced reduction of PAS$^+$ areas following transplantation of Lv.Csf2rb-transduced cells (Figure 4H).

Given the characteristic ground-glass opacities in the lungs of herPAP patients on computed tomography (CT) scans, we also performed CT scans in our mice twelve weeks after HSC-GT and quantified lung densities during the inspiratory and expiratory phases (Figure 4I-K). In line with expectations and our data from BALF analysis, CT scans confirmed significant improvements in inspiration and expiration lung densities following Lv.Csf2rb HSC-GT when compared to non-treated *Csf2rb*$^{-/-}$ mice or the Lv.GFP cohort. These radiographic data were corroborated by mechanical data of the lung demonstrating improved static compliance and inspiratory capacity in *Csf2rb*$^{-/-}$mice upon transplantation of Lv.Csf2rb-transduced cells (*Online Supplementary Figure S3B and C*).

In summary, these data demonstrate that HSC-GT employing the Lv.Csf2rb vector significantly improves and (concerning some of these parameters) even completely normalizes the herPAP disease phenotype.

Lv.Csf2rb hematopoietic stem cell-based gene therapy provides long-term cure for hereditary pulmonary alveolar proteinosis disease phenotype

To better assess the long-term potential of our HSC-GT approach, we performed serial transplantation to secondary recipients. Indeed, in half of the secondary recipients, robust pulmonary engraftment of AM associated with pronounced clinical benefit similar to primary recipients was observed indicated by decreased turbidity and

improved total protein, cholesterol, GM-CSF, M-CSF and MCP-1 levels in the BALF twelve weeks after secondary HSC-GT (Figure 5A-G). These data, in combination with the low transgene levels and VCN observed in the PB and BM of the primary recipients (Figure 3F), suggested that only some of the secondary recipients engrafted with long-term reconstituting HSC. This was supported by VCN analysis in secondary recipients, which revealed that those mice not benefitting from the transplantation had no or barely detectable VCN in their BM (VCN 0 and 0.03), in contrast to the mice presenting with an improved PAP phenotype (VCN 0.46 and 1.93) (Figure 5H). These data clearly indicate that the disease phenotype can be ameliorated in secondary recipients, in which engraftment of gene-corrected cells can be achieved.

In addition to secondary transplantation, we also performed long-term studies in primary recipients. Here, 5 of 7 mice presented AM in the range of 8 to 64% of all

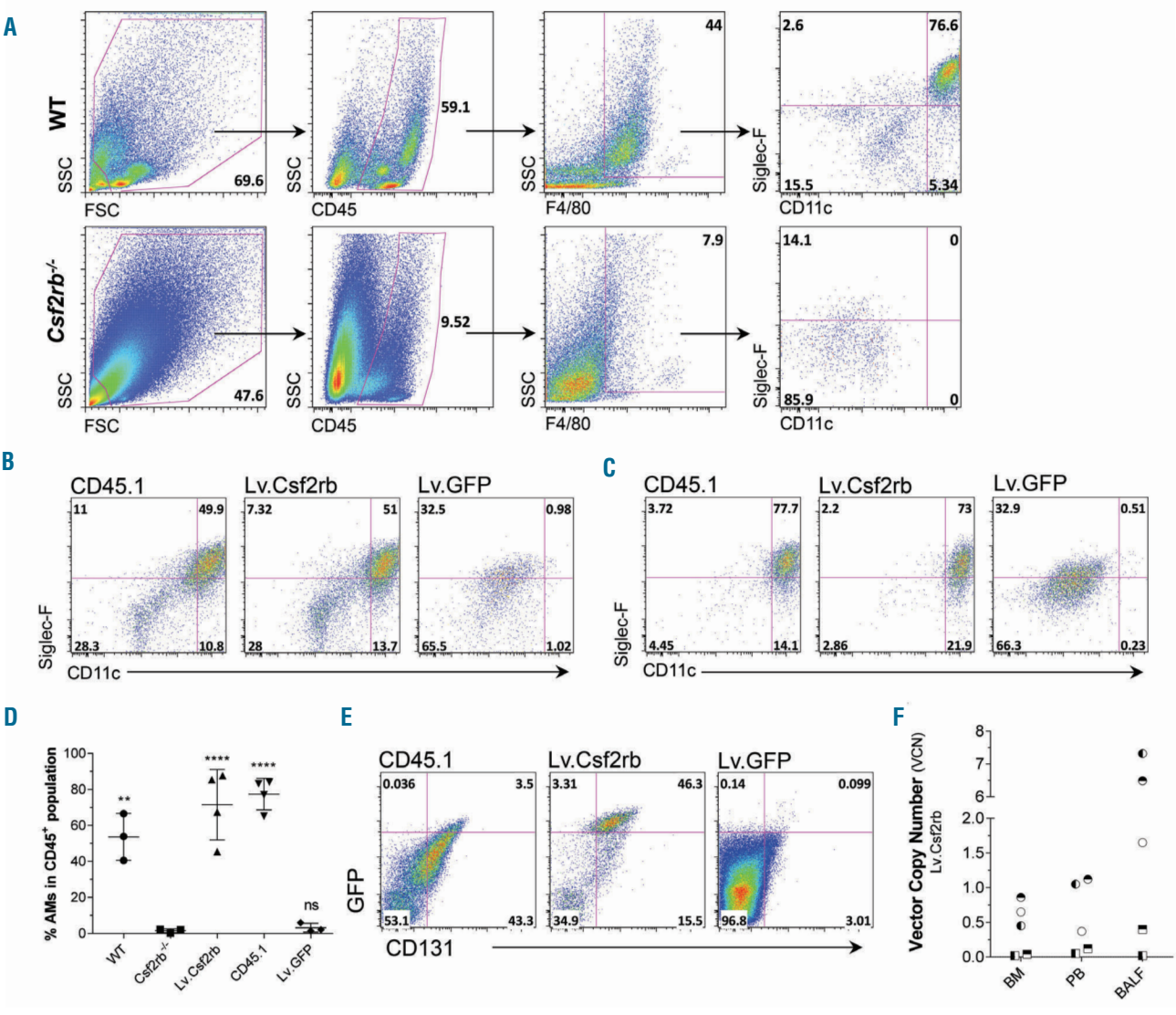

Figure 3. Lv.Csf2rb-transduced cells migrate to the lungs and reconstitute the alveolar macrophages (AM) pool upon hematopoietic stem cell-based gene therapy (HSC-GT). (A) Gating strategy for AM analysis. The first row is depicting a wild-type (WT) mouse, the second row depicts a *Csf2rb*$^{-/-}$ mouse with characteristic accumulation of events due to lipoproteinaceous material. Lung and bronchoalveolar lavage fluid (BALF) samples were pre-gated according to FSC/SSC to exclude debris (first plot). Within this population, CD45^{+} cells were gated (second plot). Out of the CD45^{+} population, all F4/80^{+} cells were gated to obtain the macrophage populations (third plot). Within the CD45^{+}F4/80^{+} population, CD11c^{high}Siglec-F^{+} represent the alveolar macrophages (fourth plot). (B) Representative pseudocolor plots of homogenized lung tissue pre-gated on CD45^{+}F4/80^{+} cells depicting the CD11c^{high}Siglec-F^{+} alveolar macrophage population in *Csf2rb*$^{-/-}$ mice transplanted with healthy CD45.1 or Lv.Csf2rb-transduced cells that is absent in mice transplanted with Lv.GFP-transduced cells. (C) Representative pseudocolor plots of BALF pre-gated on CD45^{+}F4/80^{+} cells depicting CD11c^{high}Siglec-F^{+} alveolar macrophages. (D) Percentage of AM in the total CD45^{+} population. BALF was pre-gated according to FSC/SSC to exclude debris. All CD45^{+} cells were gated and the percentage of CD11c^{high}Siglec-F^{+} cells within the total CD45^{+} population was analyzed. WT, *Csf2rb*$^{-/-}$ and Lv.GFP n=3, Lv.Csf2rb and CD45.1 n=4. Statistical analysis was carried out by one-way ANOVA with Tukey's multiple comparison testing comparing all samples to untreated *Csf2rb*$^{-/-}$ mice; ns: not significant; $^{**}P<0.01$; $^{****}P<0.0001$. (E) Representative pseudocolor plot of BALF showing GFP and CD131 expression in total CD45^{+} population. (F) Vector copy number (VCN) in bone marrow (BM), peripheral blood (PB), and BALF of *Csf2rb*$^{-/-}$ mice transplanted with Lv.Csf2rb-transduced cells twelve weeks after HSC-GT in two independent experiments (n=5). Circles belong to the first experiment, squares to the second experiment; symbols of individual mice are the same as used in Figure 2C and D.

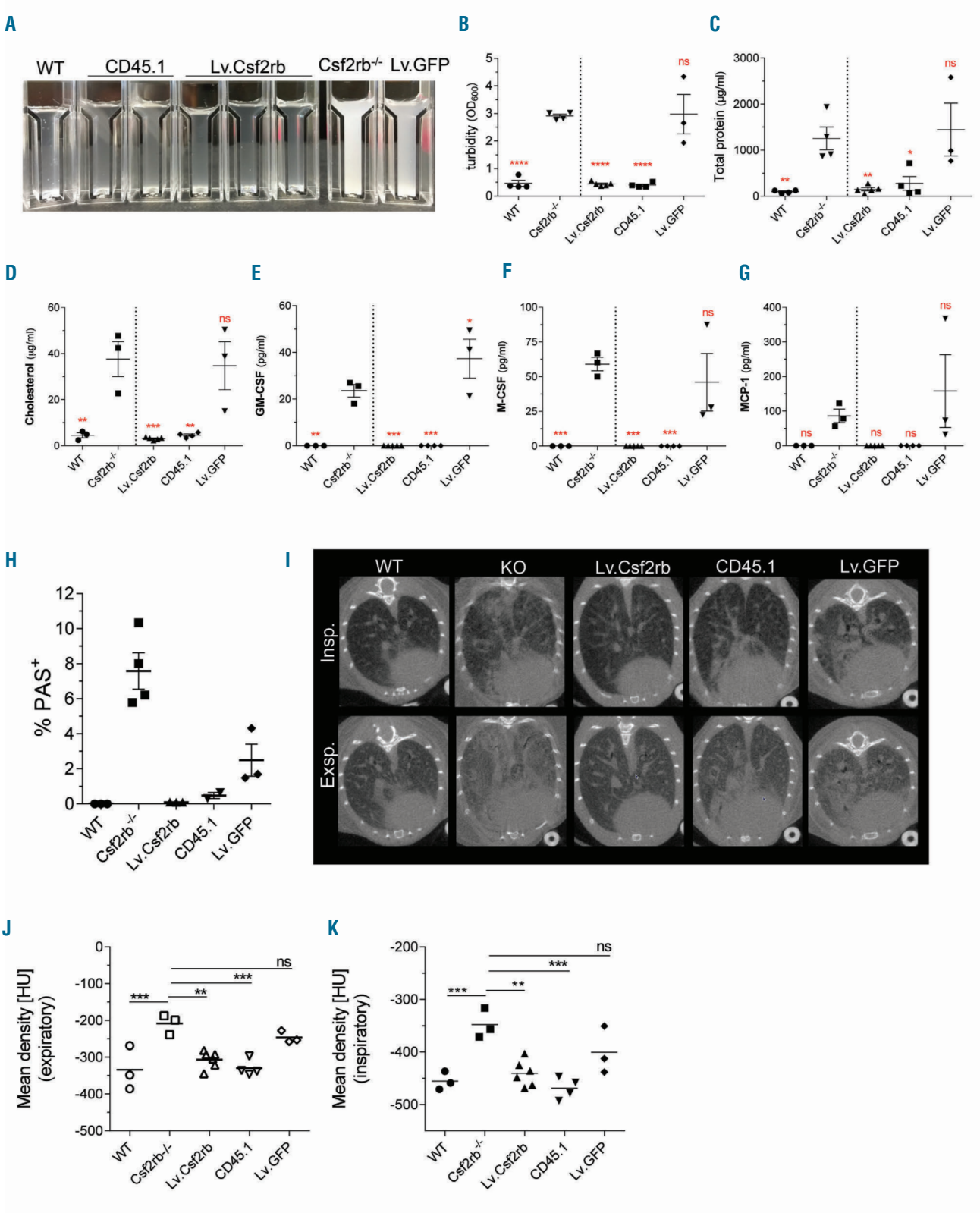

Figure 4. Significant improvement of disease-related parameters twelve weeks after Lv.Csf2rb hematopoietic stem cell-based gene therapy (HSC-GT). (A) Representative picture of bronchoalveolar lavage fluid (BALF) presenting clear and see-through fluid in untreated wild-type (WT) and *Csf2rb*$^{-/-}$ mice transplanted with healthy CD45.1 or Lv.Csf2rb-transduced cells, while *Csf2rb*$^{-/-}$ mice either untreated or transplanted with Lv.GFP-transduced cells present a hereditary pulmonary alveolar proteinosis (herPAP) characteristic milky and turbid fluid. (B) BALF turbidity measured as optical density at 600 nm (OD600). Lv.Csf2rb n=5, Lv.GFP n=3, others n=4 in two independent experiments. (C) Total protein concentration (µg/mL) in BALF. Lv.Csf2rb n=5, Lv.GFP n=3, others n=4 in two independent experiments. Cholesterol (µg/mL) (D), granulocyte/macrophage-colony-stimulating factor (GM-CSF) (pg/mL) (E), macrophage colony-stimulating factor (M-CSF) (pg/mL) (F), and monocyte chemoattractant protein-1 (MCP-1) (pg/mL) (G) levels in BALF. Lv.Csf2rb n=5, CD45.1 n=4, others n=3 in two independent experiments. (H) Quantification of Periodic Acid-Schiff (PAS) positive (PAS$^+$) areas in lung slices. Lv.Csf2rb, Lv.GFP and WT n=3, CD45.1 n=2, *Csf2rb*$^{-/-}$ n= 4. Lines indicate mean±standard error of mean. (I) Representative computed tomography scans during inspiratory (Insp.) and expiratory (Exsp.) phase. (J and K) Quantification of mean lung density in Hounsfield units (HU) measured in computed tomography scans in expiratory (J) and inspiratory (K) phase. Lv.Csf2rb n=6, WT, *Csf2rb*$^{-/-}$ and Lv.GFP n=3, CD45.1 n=4 in two independent experiments. Lines indicate means. All statistical analysis was carried out by one-way ANOVA with Dunnett's multiple comparison testing comparing all samples to untreated *Csf2rb*$^{-/-}$ mice; ns: not significant; *P<0.05; **P<0.01; ***P<0.001; ****P<0.0001.

CD45$^+$ cells in BALF (*Online Supplementary Figure S4A and B*), which was accompanied by decreased turbidity, total protein, cholesterol, GM-CSF, M-CSF and MCP-1 in BALF of these mice nine months after HSC-GT (*Online Supplementary Figure S4C-I*).

Thus, Lv.Csf2rb HSC-GT can reverse the herPAP disease phenotype and provide a long-term cure.

Rapid restoration of functional alveolar macrophages following hematopoietic stem cell transplantation

Given the efficient seeding of the lung with transplanted cells and the marked improvements in disease phenotype present already three months after HSC-GT, we next aimed to thoroughly characterize and better understand the early phases of pulmonary cell engraftment and its association with disease parameters. For these studies, lin$^-$ HSPC derived from healthy CD45.1$^+$ were utilized and transplanted intravenously into lethally irradiated *Csf2rb*$^{-/-}$ mice. The fate of CD45.1$^+$ donor cells was analyzed in PB, BM, lungs and BALF one, two, four and eight weeks after HSCT (Figure 6A). Substantial contribution of CD45.1$^+$ donor cells to the total hematopoietic pool of CD45$^+$ cells was observed for the BM already one week after HSCT and increased to >90% at the 4-week time point. However, donor cells were low in the PB (4.3±0.8%) and virtually absent in the BALF and lungs at one week, and only increased moderately at the two week time point. The contribution of donor cells to overall blood cells rapidly increased to 53±14% in the PB, 39±5% in BALF, and 41±15% in lungs at four weeks and reached 64±10% in blood, 73±5% in BALF and 67±5% in lungs eight weeks after HSCT. A more detailed characterization of these donor-derived cells in the BALF using AM typical CD11c/Siglec-F marker combination revealed that the few

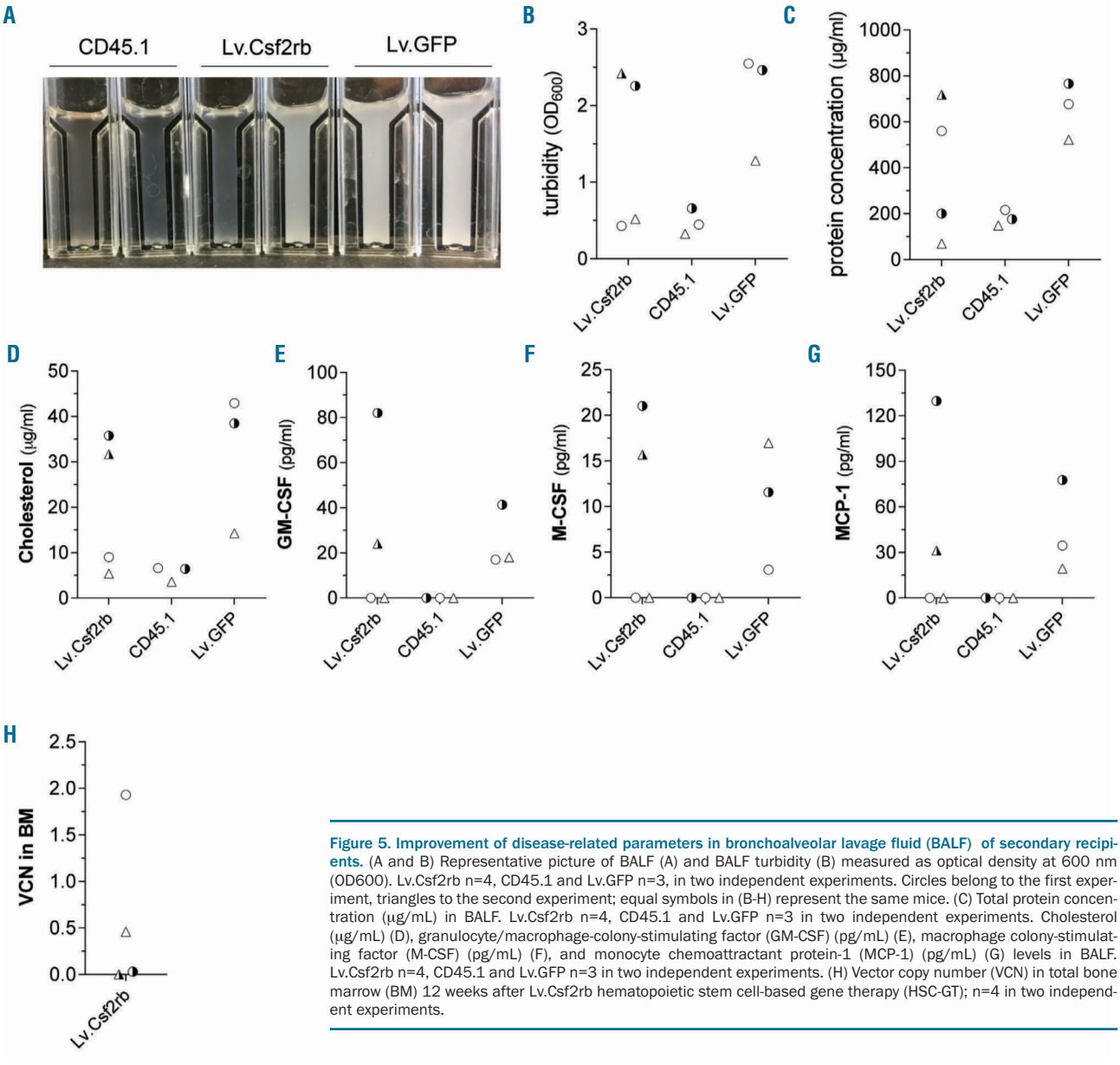

Figure 5. Improvement of disease-related parameters in bronchoalveolar lavage fluid (BALF) of secondary recipients. (A and B) Representative picture of BALF (A) and BALF turbidity (B) measured as optical density at 600 nm (OD600). Lv.Csf2rb n=4, CD45.1 and Lv.GFP n=3, in two independent experiments. Circles belong to the first experiment, triangles to the second experiment; equal symbols in (B-H) represent the same mice. (C) Total protein concentration (µg/mL) in BALF. Lv.Csf2rb n=4, CD45.1 and Lv.GFP n=3 in two independent experiments. Cholesterol (µg/mL) (D), granulocyte/macrophage-colony-stimulating factor (GM-CSF) (pg/mL) (E), macrophage colony-stimulating factor (M-CSF) (pg/mL) (F), and monocyte chemoattractant protein-1 (MCP-1) (pg/mL) (G) levels in BALF. Lv.Csf2rb n=4, CD45.1 and Lv.GFP n=3 in two independent experiments. (H) Vector copy number (VCN) in total bone marrow (BM) 12 weeks after Lv.Csf2rb hematopoietic stem cell-based gene therapy (HSC-GT); n=4 in two independent experiments.

cells present after one week were predominantly Siglec-F$^-$ CD11c$^-$ (Figure 6B). At two weeks, gradually a Siglec-F$^+$CD11c$^-$ population evolved, which persisted at week four, but after eight weeks seemed to have matured completely to a Siglec-F$^+$CD11c$^+$ AM population. Thus, eight weeks after HSCT, the mature Siglec-F$^+$CD11c$^+$ AM population was dominant and accounted for 75±2% of all CD45.1$^+$ cells. Correlating these engraftment kinetics with BALF turbidity as a critical marker of disease severity (Figure 6C and D), the occurrence of the Siglec-F$^+$CD11c$^-$ "AM progenitor-like" population two weeks after HSCT was associated with a small, though not yet significant, improvement. The occurrence of Siglec-F$^+$CD11c$^+$ AMs at weeks 4 and 8 was associated with the profound and significant reversal of the herPAP disease phenotype. This stringent correlation between the appearance of AM in the BALF and reversal of disease parameters underlines the importance of reconstitution of the AM population in the alveolar spaces as the critical factor for surfactant breakdown and disease improvements.

Discussion

Utilizing *Csf2rb*$^{-/-}$ mice, a model closely mimicking the human disease phenotype of herPAP, the current work establishes the feasibility and efficacy of an HSC-GT-based approach for the treatment of this disease entity. Two months after HSCT, we demonstrate rapid, robust and long-term seeding of the alveolar spaces with genetically repaired AM, associated with marked improvements in major disease parameters including BALF turbidity, protein content, GM-CSF, M-CSF, and cholesterol levels, pulmonary density on CT scans, alveolar deposition of PAS$^+$ material on lung histology, as well as respiratory mechanics. Concerning BALF parameters, even normalization to the levels of WT control animals was demonstrated. These data are in accordance with earlier reports on retrovirus-based HSC-GT in the *Csf2rb*$^{-/-}$ model.[9] However, these studies not only employed mutagenesis prone, LTR-driven transgene expression and a selection cassette within the vector backbone, but also fell short of a detailed

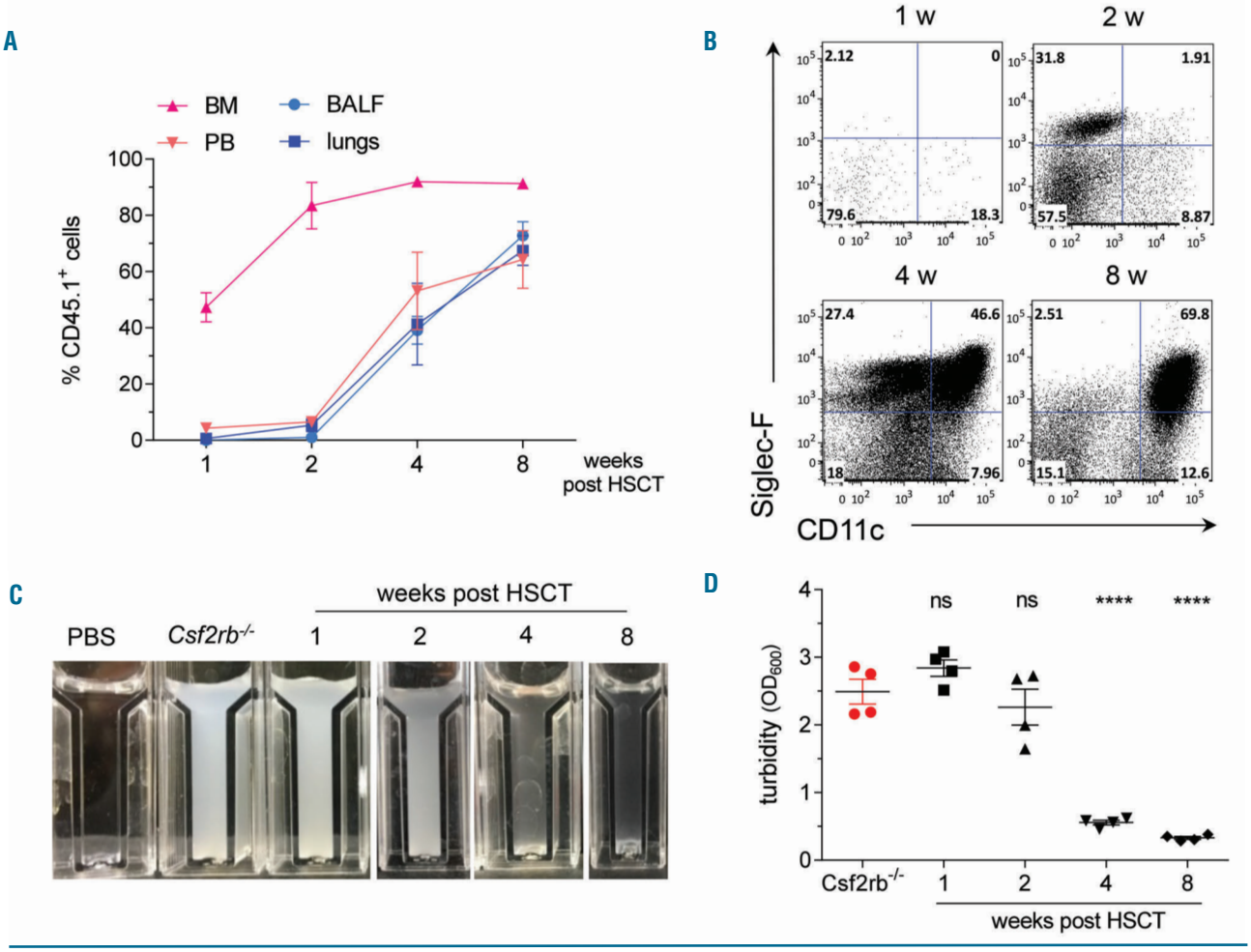

Figure 6. Rapid recovery of functional alveolar macrophages (AM) after hematopoietic stem cell transplantation (HSCT). (A) Engraftment of healthy CD45.1$^+$ donor-derived cells in bone marrow (BM), lungs, bronchoalveolar lavage fluid (BALF), and peripheral blood (PB) of *Csf2rb*$^{-/-}$ recipients one, two, four, and eight weeks (w) after HSCT. Data points indicate mean±standard error of mean (SEM); n=4 in one experiment. (B) Representative dot plots depicting expression of AM markers CD11c and Siglec-F in the CD45$^+$ fraction derived from BALF one, two, four, and eight weeks after HSCT. (C) Representative pictures of BALF derived one, two, four, and eight weeks after HSCT, untreated *Csf2rb*$^{-/-}$ mice and plain phosphate buffer saline (PBS) that was used for lavage. (D) Quantification of BALF turbidity (OD600) one, two, four, and eight weeks after HSCT. Lines and error bars indicate mean±SEM; n=4 in one experiment. Statistical analysis was carried out by one-way ANOVA with Dunnett's multiple comparison testing comparing all samples to untreated *Csf2rb*$^{-/-}$ mice; ns: not significant; **** P<0.0001.

analysis of pulmonary engraftment and the effect on the various disease parameters. Moreover, in the current study, pronounced therapeutic efficacy was shown for prolonged periods employing the 9-month time point or secondary HSCT as read-outs. Thus, our data demonstrate the profound potential of HSC-based therapies for the treatment of herPAP.

These findings have considerable relevance for the future treatment of herPAP patients. So far, therapy of herPAP patients is symptomatic only, and combines vigorous antibiotic prophylaxis and treatment of pulmonary infections with repetitive whole lung lavage, a highly invasive procedure associated with considerable cardiovascular risks.[1,3,5] Importantly, alloHSCT or HSC-GT, which meanwhile represent fairly established therapeutic concepts for other congenital diseases affecting the lymphohematopoietic system, were considered problematic in herPAP patients due to the severe lung phenotype that complicates the preconditioning procedure.[3] On the other hand, reduced-intensity conditioning regimens, improvements in diagnosis, and treatment of bacterial, fungal and viral infections, as well as better HLA-matching, have considerably advanced the field of HSCT, and successful alloHSCT has recently been described in two patients suffering from secondary PAP due to primary immunodeficiencies,[10] as well as in a herPAP patient.[11] Moreover, new therapeutic strategies for herPAP targeting cholesterol homeostasis[19,22] may ameliorate symptoms in PAP patients, and, at least in murine disease models, direct intrapulmonary transplantation of macrophages has been shown to improve substantially (if not cure) herPAP disease.[12-16] Given this, HSCT-based treatment approaches increasingly appear to be a realistic scenario, and in this context, HSC-GT avoids the critical side effects of alloHSCT such as graft-*versus*-host disease or graft rejection, and might also allow for less toxic preconditioning regimens.

In the current study, we have utilized *Csf2rb*-deficient mice primarily based on availability. However, given the almost identical clinical presentation of *CSF2RA*- and *CSF2RB*-deficient herPAP patients,[23] the HSC-GT based treatment approach presented here should apply to both molecular types of herPAP. Of note, recently also *Csf2ra*-deficient mice have been generated, and these are now available for detailed efficacy and safety testing also for *Csf2ra* expression vectors.[24,25]

In our study, we employed a 3rd generation, safety-improved SIN vector design, which is also used in current HSC-GT-based approaches targeting other monogenic diseases affecting the lymphohematopoietic system, such as X-linked- or adenosine deaminase-deficient severe combined immunodeficiency (X-SCID, ADA-SCID),[26,27] Wiskott Aldrich syndrome (WAS),[28] metachromatic leukodystrophy,[29] or hemoglobinopathies such as β-thalassemia and sickle cell disease.[30,31] Importantly, in the past, a number of phase I/II clinical studies using HSC-GT approaches and LTR-driven transgene expression suffered from insertional mutagenesis and leukemia induced by transactivation of oncogenes *via* retroviral enhancer sequences.[32-34] In contrast, modern SIN alpha-, or gamma-retroviral, as well as lentiviral vector constructs, harbor inactivating mutations in their LTR and employ internal promoters usually derived from house-keeping genes for transgene expression. Meanwhile, more than 100 patients have undergone HSC-GT employing safety modified SIN vectors, such as the one used in our study, without a single event of insertional leukemia. This covers observation periods extending up to ten years in individual patients.

In our model, low VCN in BM cells ranging from 0.02 to 0.86 were sufficient to provide pronounced clinical benefit, which represents an additional safety feature as low VCN reduce the risk of insertion-triggered mutagenic events. Moreover, it corroborates data from GM-CSFR-deficient cells where single copy *CSF2RA* expression from an EFS-driven lentiviral construct was sufficient to initiate GM-CSFR downstream signaling.[35] Interestingly, corrected cells with VCN of up to 7.32 were recruited to and enriched in the lungs, where they exerted their therapeutic effects. This observation is most likely due to the increased pulmonary cytokine levels in herPAP and the feedback mechanism by which cytokines, and in particular GM-CSF, regulate the AM pool.[23]

Recovery of the AM pool following injection of HSC occurred rapidly and resulted in an intra-alveolar cell population displaying the AM typical Siglec-F$^+$CD11c$^+$ phenotype 4-8 weeks after transplantation recapitulating the data from other murine HSC transplant models.[36,37] This time course also mimics quite well the clinical situation following alloHSCT, describing the emergence of donor type AM after 6-8 weeks.[11,38] Development of AM from Siglec-F$^-$CD11c$^-$ peripheral blood monocytes to mature Siglec-F$^+$CD11c$^+$ AM, as observed in our model, closely recapitulates the physiological development of AM from fetal monocytes in the early postnatal period. During fetal development, an intermediate pre-AM stage seems to be employed, which is no longer detectable once AM differentiation is completed.[39] Moreover, similar to early postnatal AM development, cytokines such as M-CSF, and particularly GM-CSF, play crucial roles in the generation and maintenance of the AM pool.[23,39,40] In this respect, the profound reduction of bronchoalveolar M-CSF as well as GM-CSF levels observed in our studies reflect the (auto)-regulatory reaction to the successful pulmonary engraftment and differentiation of AM. It remains unknown whether the rapid recovery of the AM compartment in our studies is due to progenitors generated in the murine BM following HSC engraftment or is achieved directly from primitive hematopoietic cells present in the graft.

Thus, in summary, we provide evidence that 3rd generation SIN lentiviral vector-based HSC-GT effectively reverses the GM-CSF-dependent disease pathology and normalizes, or at least significantly improves, critical disease-related parameters in a relevant murine model of herPAP. On these grounds, we would advocate HSC-GT as an effective and cause-directed therapeutic approach for herPAP patients, which in the clinical setting should offer the chance of long-lasting improvement of symptoms, if not a definitive cure for herPAP patients.

Acknowledgments

The authors would like to thank M. Ballmaier (Cell Sorting Facility, Hannover Medical School) for scientific support and D. Lüttge, E. Janosz, J. Mischke (Institute of Experimental Hematology, Hannover Medical School), P. Felsch, S. Eilert, and A. Kanwischer (Department of Nuclear Medicine, Hannover Medical School) for experimental and technical support.

Funding

This work was supported by grants from the Else Kröner-Fresenius-Stiftung (2013_A24 to T.M. and 2015_A92 to NL),

the Eva Luise Köhler Research Award for Rare Diseases (to GH, NL and TM), Deutsche Forschungsgemeinschaft (Cluster of Excellence REBIRTH), the German Ministry for Education and Technology (BMBF, grant 01EK1602A to GH, NL and TM), JSPS KAKENHI 16K21750 (to TS), Astellas Foundation for Research on Metabolic Disorders (to TS) and the NIH R01HL136721 (to TS) R01HL085453 (to BCT), R01HL118342 (to BCT), U54HL127672 (to BCT).

References

1. Suzuki T, Sakagami T, Young LR, et al. Hereditary pulmonary alveolar proteinosis: pathogenesis, presentation, diagnosis, and therapy. Am J Respir Crit Care Med. 2010; 182(10):1292-1304.
2. Suzuki T, Sakagami T, Rubin BK, et al. Familial pulmonary alveolar proteinosis caused by mutations in CSF2RA. J Exp Med. 2008;205(12):2703-2710.
3. Martinez-Moczygemba M, Doan ML, Elidemir O, et al. Pulmonary alveolar proteinosis caused by deletion of the GM-CSFRα gene in the X chromosome pseudoautosomal region 1. J Exp Med. 2008; 205(12):2711-2716.
4. Suzuki T, Maranda B, Sakagami T, et al. Hereditary pulmonary alveolar proteinosis caused by recessive CSF2RB mutations. Eur Respir J. 2011;37(1):201-204.
5. Tanaka T, Motoi N, Tsuchihashi Y, et al. Adult-onset hereditary pulmonary alveolar proteinosis caused by a single-base deletion in CSF2RB. J Med Genet. 2011;48(3):205-209.
6. Kaufmann KB, Buning H, Galy A, Schambach A, Grez M. Gene therapy on the move. EMBO Mol Med. 2013;5(11):1642-1661.
7. Morgan RA, Gray D, Lomova A, Kohn DB. Hematopoietic Stem Cell Gene Therapy: Progress and Lessons Learned. Cell Stem Cell. 2017;21(5):574-590.
8. Nishinakamura R, Wiler R, Dirksen U, et al. The pulmonary alveolar proteinosis in granulocyte macrophage colony-stimulating factor/interleukins 3/5 beta c receptor-deficient mice is reversed by bone marrow transplantation. J Exp Med. 1996;183(6):2657-2662.
9. Kleff V, Sorg UR, Bury C, et al. Gene therapy of beta(c)-deficient pulmonary alveolar proteinosis (beta(c)-PAP): studies in a murine in vivo model. Mol Ther. 2008;16(4):757-764.
10. Tanaka-Kubota M, Shinozaki K, Miyamoto S, et al. Hematopoietic stem cell transplantation for pulmonary alveolar proteinosis associated with primary immunodeficiency disease. Int J Hematol. 2018;107(5):610-614.
11. Fremond ML, Hadchouel A, Schweitzer C, et al. Successful haematopoietic stem cell transplantation in a case of pulmonary alveolar proteinosis due to GM-CSF receptor deficiency. Thorax. 2018;73(6):590-592.
12. Happle C, Lachmann N, Skuljec J, et al. Pulmonary transplantation of macrophage progenitors as effective and long-lasting therapy for hereditary pulmonary alveolar proteinosis. Sci Transl Med. 2014;6(250):250ra113.
13. Happle C, Lachmann N, Ackermann M, et al. Pulmonary transplantation of human Induced pluripotent stem cell-derived macrophages ameliorates pulmonary alveolar proteinosis. Am J Respir Crit Care Med. 2018;198(3):350-360.
14. Mucci A, Lopez-Rodriguez E, Hetzel M, et al. iPSC-Derived Macrophages Effectively Treat Pulmonary Alveolar Proteinosis in Csf2rb-Deficient Mice. Stem Cell Reports. 2018;11(3):696-710.
15. Takata K, Kozaki T, Lee CZW, et al. Induced-Pluripotent-Stem-Cell-Derived Primitive Macrophages Provide a Platform for Modeling Tissue-Resident Macrophage Differentiation and Function. Immunity. 2017;47(1):183-198.e6.
16. Suzuki T, Arumugam P, Sakagami T, et al. Pulmonary macrophage transplantation therapy. Nature. 2014;514(7523):450-454.
17. Nishinakamura R, Nakayama N, Hirabayashi Y, et al. Mice deficient for the IL-3/GM-CSF/IL-5 beta c receptor exhibit lung pathology and impaired immune response, while beta IL3 receptor-deficient mice are normal. Immunity. 1995;2(3):211-222.
18. Mucci A, Kunkiel J, Suzuki T, et al. Murine iPSC-Derived Macrophages as a Tool for Disease Modeling of Hereditary Pulmonary Alveolar Proteinosis due to Csf2rb Deficiency. Stem Cell Reports. 2016; 7(2):292-305.
19. Sallese A, Suzuki T, McCarthy C, et al. Targeting cholesterol homeostasis in lung diseases. Sci Rep. 2017;7(1):10211.
20. Hara T, Miyajima A. Two distinct functional high affinity receptors for mouse interleukin-3 (IL-3). EMBO J. 1992;11(5):1875-1884.
21. Iyonaga K, Suga M, Yamamoto T, Ichiyasu H, Miyakawa H, Ando M. Elevated bronchoalveolar concentrations of MCP-1 in patients with pulmonary alveolar proteinosis. Eur Respir J. 1999;14(2):383-389.
22. McCarthy C, Lee E, Bridges JP, et al. Statin as a novel pharmacotherapy of pulmonary alveolar proteinosis. Nat Commun. 2018; 9(1):3127.
23. Suzuki T, Trapnell BC. Pulmonary Alveolar Proteinosis Syndrome. Clin Chest Med. 2016;37(3):431-440.
24. Schneider C, Nobs SP, Heer AK, et al. Frontline Science: Coincidental null mutation of Csf2ralpha in a colony of PI3Kgamma$^{-/-}$ mice causes alveolar macrophage deficiency and fatal respiratory viral infection. J Leukoc Biol. 2017; 101(2):367-376.
25. Shima K, Suzuki T, Arumugam P, et al. Pulmonary Macrophage Transplantation Therapy in Csf2ra Gene-Ablated Mice: A Novel Model of Hereditary Pulmonary Alveolar Proteinosis in Children. In: B108. CYSTIC FIBROSIS, PRIMARY CILIARY DYSKINESIA, AND ILD. American Thoracic Society; 2017. p. A4857.
26. De Ravin SS, Wu X, Moir S, et al. Lentiviral hematopoietic stem cell gene therapy for X-linked severe combined immunodeficiency. Sci Transl Med. 2016;8(335):335ra57.
27. Gaspar HB, Buckland K, Rivat C, et al. 276. Immunological and metabolic correction after lentiviral vector mediated haematopoietic stem cell gene therapy for ADA deficiency. Molecular Therapy. 2014;22:S106.
28. Aiuti A, Biasco L, Scaramuzza S, et al. Lentiviral hematopoietic stem cell gene therapy in patients with Wiskott-Aldrich syndrome. Science. 2013;341(6148):1233151.
29. Biffi A, Montini E, Lorioli L, et al. Lentiviral hematopoietic stem cell gene therapy benefits metachromatic leukodystrophy. Science. 2013;341(6148):1233158.
30. Cavazzana-Calvo M, Payen E, Negre O, et al. Transfusion independence and HMGA2 activation after gene therapy of human beta-thalassaemia. Nature. 2010;467(7313):318-322.
31. Kanter J, Walters MC, Hsieh M, et al. Interim results from a Phase 1/2 clinical study of lentiglobin gene therapy for severe sickle cell disease. Blood. 2017;130(Suppl 1):527-527.
32. Hacein-Bey-Abina S, Garrigue A, Wang GP, et al. Insertional oncogenesis in 4 patients after retrovirus-mediated gene therapy of SCID-X1. J Clin Invest. 2008;118(9):3132-3142.
33. Hacein-Bey-Abina S, Von Kalle C, Schmidt M, et al. LMO2-associated clonal T cell proliferation in two patients after gene therapy for SCID-X1. Science. 2003;302(5644):415-419.
34. Stein S, Ott MG, Schultze-Strasser S, et al. Genomic instability and myelodysplasia with monosomy 7 consequent to EVI1 activation after gene therapy for chronic granulomatous disease. Nat Med. 2010;16(2):198-204.
35. Hetzel M, Suzuki T, Hashtchin AR, et al. Function and safety of lentivirus-mediated gene transfer for CSF2RA-deficiency. Hum Gene Ther Methods. 2017;28(6):318-329.
36. Matute-Bello G, Lee JS, Frevert CW, et al. Optimal timing to repopulation of resident alveolar macrophages with donor cells following total body irradiation and bone marrow transplantation in mice. J Immunol Methods. 2004;292(1-2):25-34.
37. Murphy J, Summer R, Wilson AA, Kotton DN, Fine A. The prolonged life-span of alveolar macrophages. Am J Respir Cell Mol Biol. 2008;38(4):380-385.
38. Nakata K, Gotoh H, Watanabe J, et al. Augmented proliferation of human alveolar macrophages after allogeneic bone marrow transplantation. Blood. 1999;93(2):667-673.
39. Guilliams M, De Kleer I, Henri S, et al. Alveolar macrophages develop from fetal monocytes that differentiate into long-lived cells in the first week of life via GM-CSF. J Exp Med. 2013;210(10):1977-1992.
40. Hashimoto D, Chow A, Noizat C, et al. Tissue-resident macrophages self-maintain locally throughout adult life with minimal contribution from circulating monocytes. Immunity. 2013;38(4):792-804.